Mimics and Pitfalls in Renal Imaging

Erick M. Remer, MD

KEYWORDS

• Technical pitfall • Phase of contrast enhancement • Region of interest • Renal pseudotumor • Fat-containing renal mass

KEY POINTS

- Not all focal renal abnormalities are malignant tumors; benign neoplasms and posttraumatic, infectious, vascular, and treatment changes can mimic malignancy.
- Attention to technical details when interpreting renal images is paramount; radiologists must consider factors such as the imaging protocol, imaging plane, phase of enhancement, and region-of-interest placement.
- Identification of fat within a renal mass and characterization of the type of fat can narrow the differential diagnosis.

INTRODUCTION

In general terms, much of what we do when characterizing renal lesions involves a binary determination: an abnormality either enhances and is thus more likely to be a tumor or does not enhance and is thus more likely to be a benign lesion. However, there are many instances in which these simplistic rules do not apply. In such cases, clues to making the correct diagnosis may be historical (such as the presence of pyuria and fever or a history of renal trauma or surgery) or may relate to specific imaging features of a focal abnormality (such as shape or the presence of intralesional fat). Further, several technical pitfalls may be encountered when interpreting renal images. These pitfalls may be related to contrast delivery, phase of enhancement, or collecting system opacification after contrast administration; imaging plane orientation with respect to a renal abnormality; use of proper window and level settings during image interpretation; and placement of regions of interest (ROIs) to measure attenuation or signal intensity. In addition, several focal renal lesions can mimic tumors. These pseudotumors may be congenital, may have a vascular origin, may result from prior infection or trauma, or may be related to therapy for renal cell carcinoma (RCC) such as partial nephrectomy or tumor ablation. Finally, the detection of either microscopic or macroscopic fat within renal masses affects the differential diagnosis, and so appropriate methods must be used to detect fat and interpret the resulting images. This article reviews these potential pitfalls in renal imaging.

TECHNICAL PITFALLS

Technical pitfalls in renal imaging may be patient related, image acquisition related, or interpretation related (**Table 1**). When patients move or fail to hold their breath during image acquisition, attenuation measurements may be spuriously increased or decreased, and image degradation and blurring may occur. These misregistration artifacts usually seem as shading or streaking in the reconstructed image.[1]

Sometimes, renal abnormalities may be less well depicted or difficult to identify based on their position in the kidney with respect to the imaging plane. For example, a renal mass in the upper or lower pole may be easily scrolled past when

Imaging Institute and Glickman Urological and Kidney Institute, Cleveland Clinic, 9500 Euclid Avenue, A21, Cleveland, OH 44195, USA
E-mail address: remere1@ccf.org

Radiol Clin N Am 58 (2020) 885–896
https://doi.org/10.1016/j.rcl.2020.05.001

Table 1
Technical pitfalls

Element	Description
Motion	Spurious increased or decreased attenuation
Window level settings	Altered lesion detectability
Imaging plane with respect to lesion location	Decreased lesion visibility in some planes vs in others
Phase of contrast	Diminished detectability in corticomedullary phase
Pseudoenhancement	Spurious increased attenuation in contrast-enhanced phase vs in unenhanced phase

viewed on the PACS workstation but may be more obvious to the reader when visualized in the coronal or sagittal plane (Fig. 1). Multiplanar reformatted images can improve the reader's confidence in the identification of small masses that more clearly deform the renal contour when viewed in one plane than in another.[2] A study that assessed missed imaging findings by radiology residents found that 5.5% of missed findings on abdomen and pelvic computed tomographic (CT) images were cases of pyelonephritis and that residents believed that the use of coronal images would help to provide a thorough evaluation of the renal cortices.[3]

The phase of contrast during which imaging occurs can also greatly affect the detectability of renal masses. One study found that nephrographic phase images, when compared with medullary phase images, can show 1.3 times more masses in the renal cortex[4] and 4 to 5 times more masses in the medulla[3,5] (Fig. 2). Although the phases of renal enhancement may vary based on the rate of delivery of contrast material, generally speaking, the corticomedullary phase occurs approximately 30 to 40 seconds after the beginning of contrast administration and the nephrographic phase begins at 80 to 120 seconds.[6] Because the speed of CT scanners has increased, the kidneys are now often visualized during the corticomedullary phase on single-phase, routine abdominal protocol CT scans. Small hyperenhancing clear cell RCCs (ccRCCs) can be particularly difficult to detect during this phase, as these lesions may be isoattenuating to normal parenchyma in the corticomedullary phase and may only be discernible based on subtle interruption of normal corticomedullary enhancement or heterogeneous tumor enhancement (Fig. 3).

Another technical pitfall encountered in renal imaging is the phenomenon of pseudoenhancement, which involves mischaracterizing a renal cyst as an enhancing neoplasm because of a false attenuation change between unenhanced and enhanced images. Pseudoenhancement is thought to be the result of multidetector, spiral CT image reconstruction algorithms that adjust for beam-hardening effects.[7] Several factors may affect the degree of pseudoenhancement, including lesion size or location, degree of renal parenchymal enhancement, number of CT detector rows, peak tube voltage, and reconstruction kernel.[8] This phenomenon tends to occur most notably with small (<1 cm) and intraparenchymal lesions (Fig. 4). If pseudoenhancement is suspected, ultrasound imaging or MR imaging can be used to determine whether the mass is truly cystic or solid.

REGION-OF-INTEREST PLACEMENT AND INTERPRETATION

The placement and interpretation of ROI attenuation measurements for the evaluation of renal masses can also be problematic. The most

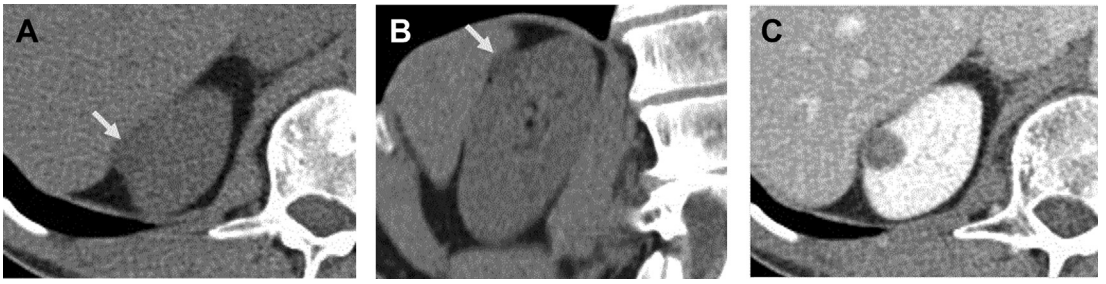

Fig. 1. (*A*) Axial unenhanced CT of right kidney shows barely discernible upper pole pRCC (*arrow*) that is more obvious (*arrow*) on coronal unenhanced multiplanar reformatted (MPR) (*B*) and axial-enhanced images (*C*).

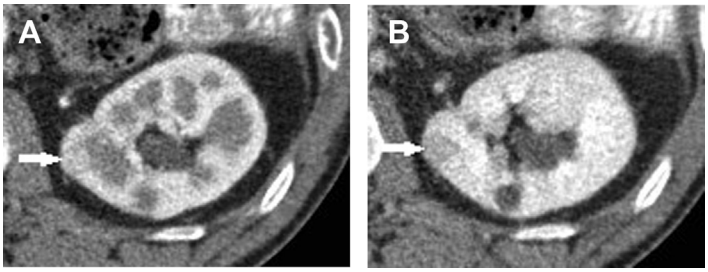

Fig. 2. (*A*) Corticomedullary phase and (*B*) nephrographic phase axial contrast-enhanced CT images of the left kidney show improved detectability of 1.2-cm ccRCC (*arrows*) when there is greater enhancement difference between the tumor and renal cortex in the nephrographic phase.

fundamental pitfall is using visual inspection alone to assess the attenuation of a renal lesion. One's eye can be tricked by homogeneous low-attenuation solid lesions mimicking cysts, so routine ROI use and proper placement is essential. Radiologists should ensure that the ROIs are placed well within the boundaries of the renal mass to avoid volume averaging with normal renal parenchyma. In addition, if the image slice thickness is less than one-half of the lesion diameter, normal parenchyma cephalad or caudad to the lesion can be volume averaged into the ROI, artificially altering it.

ROIs are placed on renal abnormalities to determine a lesion's attenuation, to assess for attenuation change between unenhanced and enhanced images (enhancement), or to detect fat within a lesion. Heterogeneity of renal lesions and the impact on ROI measurements can affect interpretation, leading to erroneous conclusions in several ways. On unenhanced CT, if a focal lesion measures less than 20 HU, has no wall thickening, is homogeneous, has no or minimal calcifications, and has no or few septa, it can be considered benign.[9,10] Discernment of heterogeneity is important to detect the uncommon RCC that measures less than 20 HU (**Fig. 5**).[11] In one series, RCC was found in approximately 0.5% of more than 15,000 patients, and 37% of these lesions were missed on initial interpretation, especially when the lesions were smaller than 3 cm.[12]

Typical papillary RCCs (pRCCs) are hyperattenuating to renal parenchyma on unenhanced scans, enhance only modestly, and tend to be homogeneous.[13–15] Rarely those with lower unenhanced attenuation values can mimic renal cysts on unenhanced CT scans. One study[16] found that of 114 pRCCs, 3 were homogeneous and measured less than 20 HU on unenhanced scans (**Fig. 6**). In another series, 24 of 104 RCCs (both ccRCCs and pRCCs) measured less than 20 HU when an ROI encompassing most of the lesion was used. However, of these 24 lesions, 21 were heterogeneous, and small ROIs could be used to detect regions within these lesions measuring more than 20 HU in the 3 that were homogeneous.[17]

If a lesion demonstrates high attenuation on an unenhanced CT image, assessment for homogeneity is again of paramount importance. The attenuation of hemorrhagic cysts and RCC can overlap on unenhanced CT images. However, if a lesion is both homogeneous and measures 70 HU or greater, it is almost certainly benign,[18] representing a hemorrhagic cyst (**Fig. 7**).

Detection of enhancement in pRCCs can be difficult, as these lesions tend to enhance only modestly.[12–14] In one series, a substantial number of pRCCs showed no CT enhancement (17% [7/41]) or equivocal enhancement (9.8% [4/41]) (**Fig. 8**).[13] Another series found that 25% of malignant lesions characterized as Bosniak III cysts

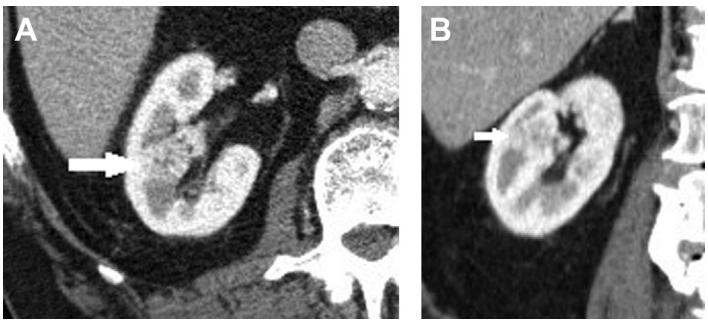

Fig. 3. (*A*) Axial and (*B*) coronal corticomedullary phase contrast-enhanced CT images of the right kidney show a ccRCC (*arrows*) that is difficult to detect because its attenuation is similar to that of the surrounding medullary renal parenchyma. One clue to the correct diagnosis is the heterogeneity of enhancement.

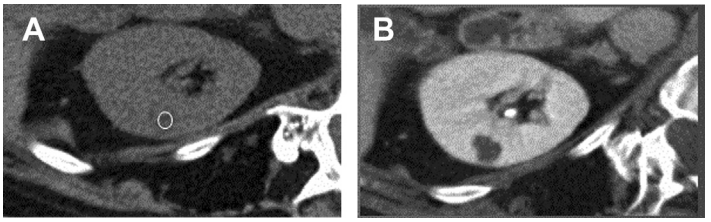

Fig. 4. Pseudoenhancement can occur when small intracortical cysts are mischaracterized as enhancing tumors. (*A*) Unenhanced and (*B*) enhanced images of the right kidney show an ROI (*circle*) used to measure the attenuation of a renal cyst before (*A*) and (*B*) after contrast administration. The unenhanced attenuation was 9 HU and the postcontrast attenuation was 30 HU, erroneously suggesting a mildly enhancing tumor.

were pRCCs.[19] This may, in part, be explained by the pathologic features of cystic change or necrosis in pRCC.[10,20] For such marginally enhancing tumors, the use of small ROIs rather than medium or large ROIs to detect enhancement has been shown to provide superior performance.[8] More particularly, researchers found that in lesions lacking enhancement that could be identified by visual observation alone, small ROIs performed statistically significantly better than whole-lesion ROIs in distinguishing any RCC from a cyst (area under the receiver operating characteristic curve [AUC]: small ROI, 0.792; whole-lesion ROI, 0.602) and in distinguishing between pRCC and a cyst (AUC: small ROI, 0.883; whole lesion ROI, 0.642) (**Fig. 9**).[8]

Because of challenges with the interpretation of CT for minimally enhancing renal masses, MR imaging can be used to problem solve by aiding in delineating tumor types and specifically identifying enhancing tissue.[21] In addition, machine learning has also been investigated as a method to differentiate between renal neoplasms and cysts; the detection of high entropy on CT texture analysis has been found to be comparable to the assessment of expert readers and superior to the assessment of novice readers in distinguishing between low-attenuation RCCs and cysts, with a sensitivity of 84% and a specificity of 80%.[22]

On contrast-enhanced CT images, a homogeneous lesion with attenuation less than 20 HU is almost certainly a cyst.[23] Emerging data from small series suggest that the attenuation threshold for benign lesions could potentially be increased to 30 or 40 HU,[24–26] with the caveat that a pRCC may rarely be missed using this new threshold.[16]

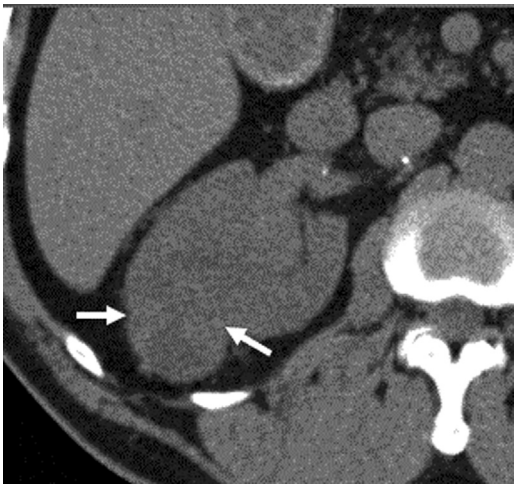

Fig. 5. Unenhanced axial CT image demonstrating poorly defined ccRCC. Although some portions measure less than 20 HU, there are areas of heterogeneous higher attenuation (*arrows*).

PSEUDOTUMORS

Several masslike renal abnormalities detected on imaging are not RCCs. When first approaching a renal abnormality, it is therefore good practice for the radiologist to question whether the finding could be developmental, posttraumatic, infectious or postinfectious, vascular, or postprocedural in origin (**Box 1**).

Congenital anatomic variants include a prominent column of Bertin, which occurs as a result of incomplete resorption of junctional parenchyma during organogenesis. This variant seems as a tongue of tissue extending into the renal sinus in contiguity with renal parenchyma. Enhancement that is similar to the surrounding parenchyma (for CT, MR imaging, or contrast-enhanced ultrasound) or uptake on cortical agent radioisotope imaging and characteristic morphology are clues to the diagnosis of this anatomic variant. In the corticomedullary phase of enhancement, a normal corticomedullary pattern also helps to distinguish potential anatomic variants from real lesions. For instance, a dromedary hump is a focal protrusion of parenchyma in the lateral midleft renal parenchyma adjacent to the spleen that should, otherwise, follow the imaging characteristics of the remainder of renal parenchyma.

Inflammatory masses such as focal pyelonephritis (**Fig. 10**), immunoglobulin G-4 (IgG4) renal

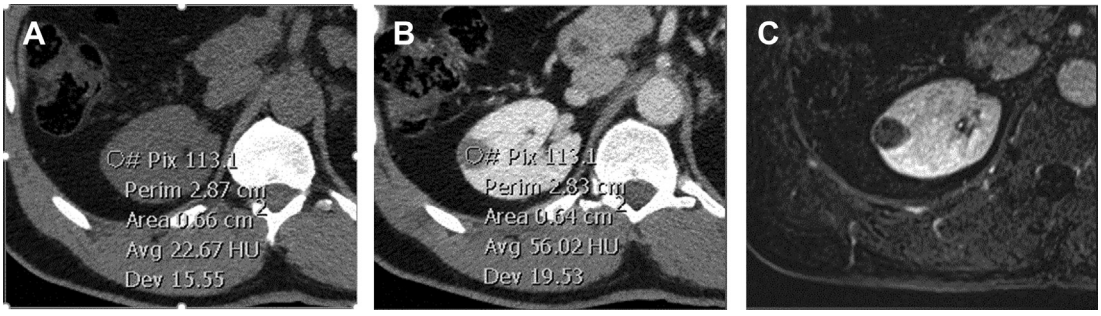

Fig. 6. Images of homogeneous low-attenuation pRCC. (*A*) ROI on unenhanced axial CT image shows a lesion attenuation of 22 HU. (*B*) Contrast-enhanced axial CT image shows a mass with an enhancement of 56 HU. (*C*) Same tumor on MR imaging with faint visual enhancement is confirmed on subtracted postcontrast axial T1-weighted fat-suppressed image.

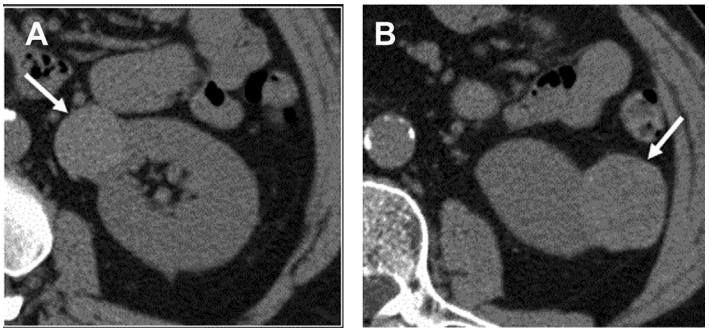

Fig. 7. Unenhanced axial CT images from a 57-year-old woman with 2 left renal masses. (*A*) Hyperdense cyst is homogeneous and measures 72 HU (*arrow*). (*B*) pRCC is mildly heterogeneous, has angular margins, and measures 58 HU (*arrow*).

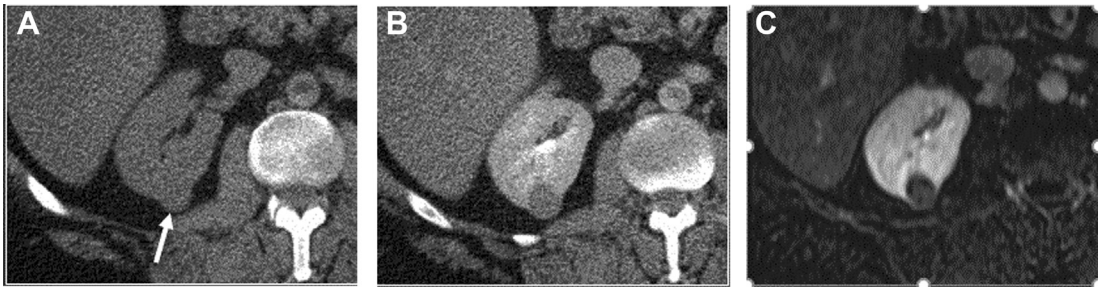

Fig. 8. Images of pRCC. (*A*) Axial unenhanced CT image shows a renal mass that measures 31 HU (*arrow*). (*B*) Nephrographic phase–enhanced axial CT image shows a mass with an attenuation of 42 HU. (*C*) Subtracted contrast-enhanced T1-weighted axial MR image of the same tumor shows minimal detectable enhancement.

disease, and abscess may have the appearance of a focal neoplasm. Combing the medical record for pertinent clinical clues can keep the radiologist from wandering down the wrong diagnostic path. For instance, focal compensatory hypertrophy or renal cortical preservation in the setting of extensive renal scarring after infection or infarction can have a masslike appearance (**Fig. 11**). After an acute inflammatory event, imaging clues to the correct diagnosis include multifocal areas of scarring, preserved corticomedullary differentiation, and stability over time.

Similarly, vascular malformations such as aneurysms or arteriovenous fistulas may appear masslike on unenhanced images or during certain phases of contrast administration. Confirmation of a vascular cause of the finding can be made with arterial phase imaging or Doppler ultrasound.

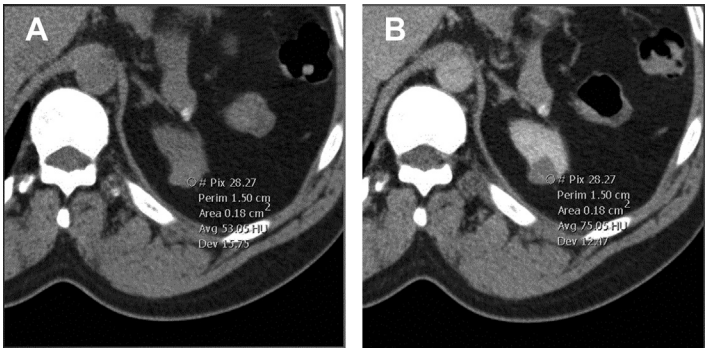

Fig. 9. Use of small ROIs to detect enhancement. (*A*) Hyperdense pRCC on unenhanced axial CT image with a small ROI demonstrates an attenuation of 53 HU. (*B*) Nephrographic phase CT image ROI measures an attenuation of 75 HU, confirming enhancement (>20 HU difference). ROIs encompassing two-thirds of the mass measured attenuation values of 55 HU and 64 HU and were, thus, unable to detect enhancement.

Findings on imaging after partial nephrectomy or renal tumor ablation can mimic findings of a residual or recurrent tumor. The resection approach used for renal tumors depends on tumor size and tumor location within the kidney with respect to the collecting system and vascular structures; these factors affect the amount of parenchyma that must be resected. Preserved renal function after resection is strongly correlated with preserved parenchymal mass and renal reconstruction, so preservation of normal renal parenchyma is imperative.[27,28] The renal remnant will have different appearances based on the amount of parenchyma that was resected and the method of renorrhaphy to achieve hemostasis closure of the renal capsule. Often, the renal capsule is reapproximated over bolsters of oxidized cellulose or other hemostatic agents, which can appear masslike, especially in the immediate postoperative period.[29]

Typically, imaging should not be performed in the immediate postoperative period unless a complication (such as hematoma with or without pseudoaneurysm, urinoma, or abscess) is suspected. Oxidized cellulose can mimic an abscess at the resection site, as it may have the appearance of a water attenuation collection with gas bubbles interspersed within it even if uninfected (**Fig. 12**).[30] A renal parenchymal defect, perinephric fat infiltration, and fluid collections (75%) are other common findings after renal mass resection.[31] Some postoperative patients will have round or ovoid mildly enhancing residual tissue at the resection site; this is usually referred to as a pseudotumor[32] or granuloma (**Fig. 13**).[33] Generally, this tissue involutes over time. Although the American Urologic Association guidelines recommend follow-up for T1 renal tumors (up to 7 cm localized to the kidney),[34] early recurrence is rare and postoperative imaging findings can be confusing. Based on these factors, the investigators of one study suggested that imaging might be best deferred until 1 year after surgery.[35]

Box 1
Types of pseudotumors

- Congenital (column of Bertin, dromedary hump)
- Masslike compensatory hypertrophy (multifocal scarring)
- Inflammatory (pyelonephritis, abscess, IgG4 disease)
- Vascular abnormality—aneurysm/pseudoaneurysm
- Partial nephrectomy pseudotumor/granuloma
- Oxidized cellulose pseudoabscess
- Early postablation enhancement

When imaging is performed later after partial nephrectomy, normal changes may be difficult to distinguish from tumor recurrence. The investigators of one small series suggested that the degree of enhancement, morphology of imaging findings, and temporal change can be used to distinguish tumor recurrence from scarring after partial nephrectomy.[36] In this study, recurrent tumors (presumably ccRCC) had greater enhancement than scarring (median 119 HU vs 48 HU) and showed enhancement loss in the nephrographic and excretory phases as opposed to increased enhancement for scarring. Also, the true recurrent tumors appeared as spiculated masses rather than as thin spidery projections and increased rather than decreased in size over time (**Fig. 14**).

Imaging findings after ablation will also vary over time. Shortly after either radiofrequency ablation or cryoablation, the treatment zone should be larger than the original tumor, because a margin of normal parenchyma is intentionally ablated. The ablation zone does not typically enhance and should decrease in size over time.[37] However, early residual enhancement in the first few days

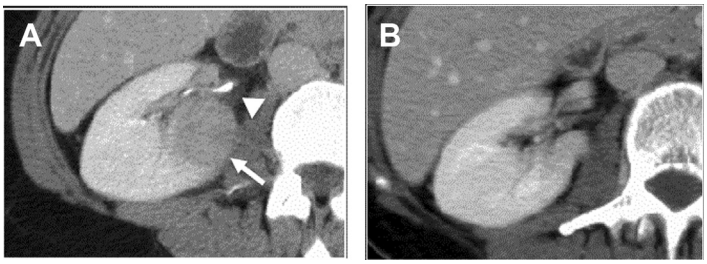

Fig. 10. (*A*) Axial contrast-enhanced CT image in a patient with flank pain shows a focal rounded masslike abnormality (*arrow*) with mild stranding in perirenal fat (*arrowhead*). The mass was initially interpreted as a neoplasm until information about pyuria and fever became available. (*B*) A follow-up–enhanced CT image obtained 4 months later shows resolution of focal infectious nephritis.

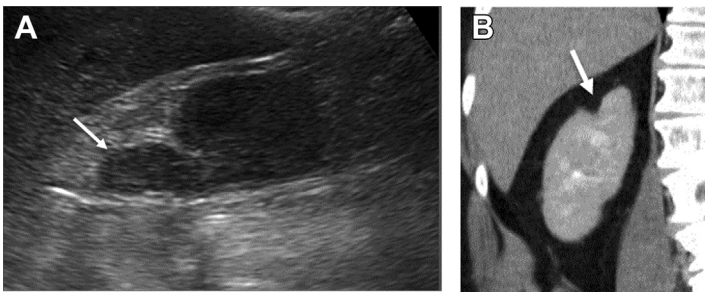

Fig. 11. A 73-year-old man with urinary obstruction. (*A*) Sagittal ultrasound image of the right kidney shows bulbous protrusion from the upper pole of the kidney (*arrow*). (*B*) Coronal contrast-enhanced CT MPR image shows that the region represents normal parenchyma adjacent to a parenchymal scar (*arrow*).

Fig. 12. Oxidized cellulose placed at renal tumor resection site (*white arrow*) is visualized as a low-attenuation collection with interspersed gas foci, mimicking an abscess on the enhanced CT image. A surgical drain (*black arrow*) can also be seen.

after ablation can be detected at the site of the tumor in 60% to 80% of ablation zones (**Fig. 15**).[38–40] This early enhancement, which may be homogeneous or curvilinear, occurs more commonly in cases of ccRCC and typically resolves within a month. Therefore, many centers have abandoned the use of early imaging to assess for ablation completeness, waiting until 3 months after the procedure to begin imaging follow-up.

When disease progression (recurrence) after tumor ablation does occur, it is most common at the periphery of the ablation site, has variable morphology depending on the ablation method and device, and is characterized by new nodular enhancement or internal enhancement.[31] Comparing postablation images with preablation images is extremely beneficial, as information on the exact site and morphology of the original tumor is crucial for proper interpretation of postablation images (**Fig. 16**).

FAT-CONTAINING RENAL MASSES

Some renal masses contain fat, which can aid in making a correct diagnosis based on imaging findings. However, the amount of fat, its location with respect to the cellular makeup of the lesion, and the method of detection all contribute to the complexity of deciphering and categorizing renal masses that contain fat.

The prototypical fat-containing renal mass is the angiomyolipoma (AML), a benign neoplasm that contains components of vascular tissue, smooth muscle, and adipocytes or fat cells. Most of the AMLs thus have macroscopic fat[41] (sometimes referred to as bulk fat), indicating an adequate number of adipocytes to be detected by imaging. Detection of macroscopic fat can be accomplished by finding an ROI on unenhanced CT that measures less than −10 HU.[42] For tiny foci of fat, thin-section CT reconstruction can improve sensitivity.

Fig. 13. Images of pseudotumor after partial nephrectomy. (*A*) CT image obtained 2 months after surgery shows mildly enhancing soft tissue at the resection site (*arrow*) that diminishes by 6 months (*B*) and resolves thereafter (7 years) (*C*).

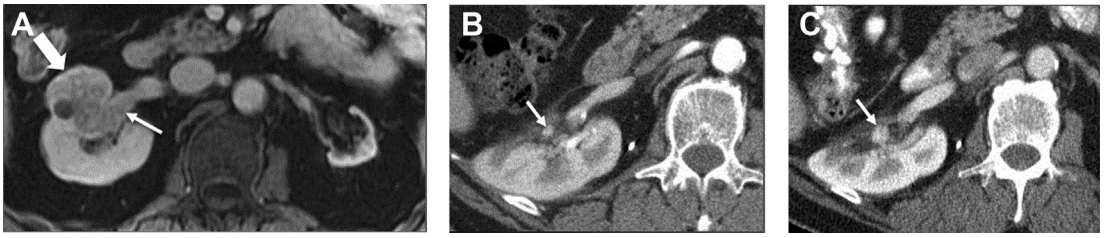

Fig. 14. (*A*) Contrast-enhanced T1-weighted MR image from a 67-year-old man with atrophic left kidney and right renal tumor (*large arrow*) with renal vein invasion (*small arrow*) treated with preoperative pazopanib followed by partial nephrectomy. (*B*) One-year follow-up CT image shows a 5-mm enhancing nodule (*arrow*) at the resection site, not identified by the interpreting radiologist. (*C*) Two-year follow-up CT image shows increase in size of nodule (*arrow*) to 1.2 cm. The patient underwent cryoablation for recurrence. Recurrent disease most commonly demonstrates rounded, convex margins, may hyperenhance (in cases of ccRCC), and increases in size over time.

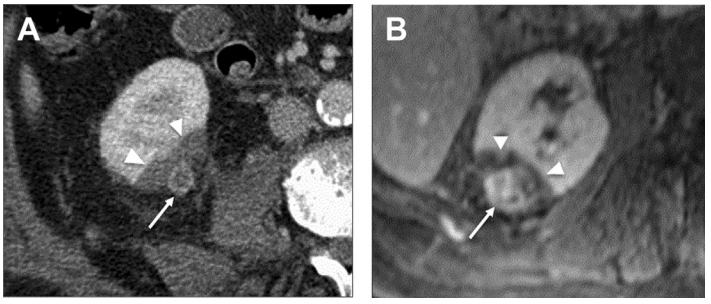

Fig. 15. Early postablation enhancement in 2 patients. (*A*) CT image obtained 1 day after ablation shows small rounded focus of enhancement (*arrow*) within ablation zone (*arrowheads*). (*B*) MR image obtained 1 day after ablation shows large rounded focus of enhancement (*arrow*) within ablation zone (*arrowheads*).

Macroscopic fat on MR imaging can be identified using several methods. Signal intensity loss after the application of chemical selective fat suppression or fat and water separation Dixon techniques can confirm the presence of macroscopic fat. Alternatively, curvilinear or linear chemical shift artifact (of the second kind) causes an India-ink artifact at the boundary of a macroscopic fat-containing lesion on T1-weighted gradient-recalled echo images. Central high signal intensity should be maintained, matching the signal intensity of other macroscopic fat (such as retroperitoneal or subcutaneous fat) and thus confirming the presence of macroscopic fat (**Fig. 17**).[35] Research has shown that MR imaging may be more sensitive to fat than unenhanced CT in small AMLs.[43]

Not all renal masses with macroscopic fat are AMLs. Rarely, macroscopic fat can be seen in RCCs, most often with coexistent calcifications.[35] When a renal mass engulfs retroperitoneal fat, leading to intralesional macroscopic fat, RCC should be suspected.

Fig. 16. Recurrence after cryoablation. (*A*) Preprocedural sagittal reformatted CT image shows small lower pole tumor (*arrow*). (*B*) Six-month fat-saturated T1-weighted sagittal MR image after cryoablation shows a normal finding of thin rim enhancement at the ablation zone boundary (*arrow*) without other enhancement. (*C*) Two-year sagittal MR image shows rounded, enhancing nodule (*arrow*) at the deep margin of the ablation zone extending into the central sinus indicating tumor recurrence.

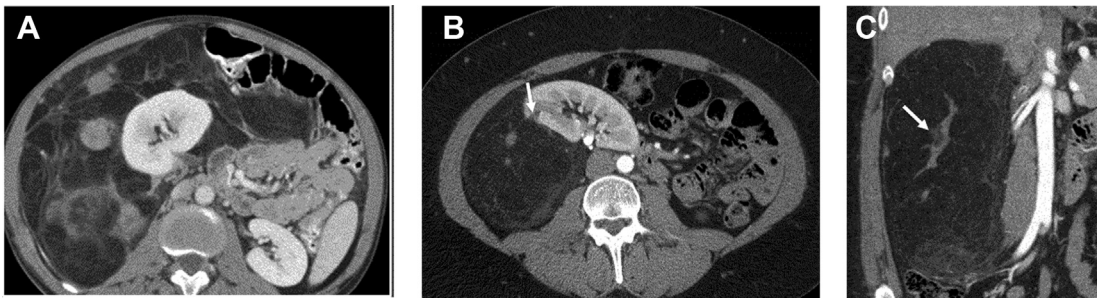

Fig. 17. Liposarcoma versus large AML. (*A*) CT image of dedifferentiated retroperitoneal liposarcoma with abundant fat and soft tissue nodules. (*B*) Large AML also appears as predominantly fat attenuation but also demonstrates a tiny renal parenchymal notch (*arrow*) and (*C*) has large central vessels (*arrow*).

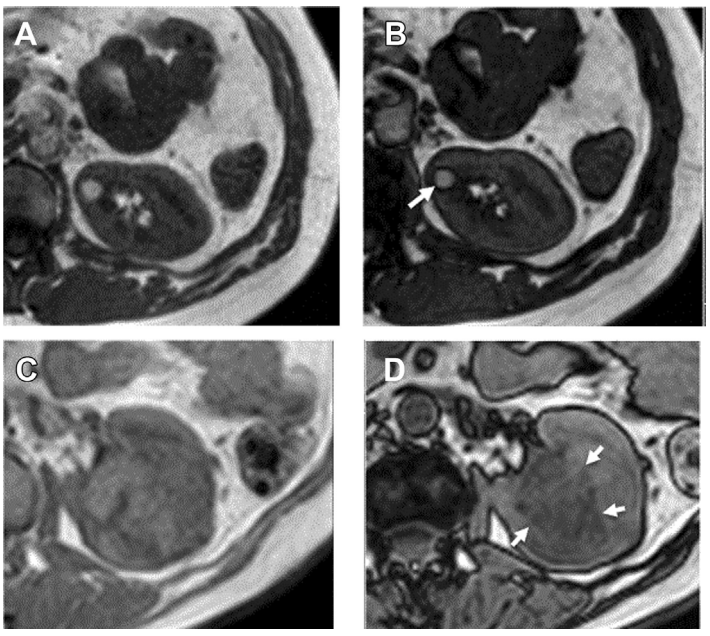

Fig. 18. Microscopic versus macroscopic fat on in-phase and opposed-phase T1-weighted gradient-recalled echo MR imaging. (*A*) In-phase and (*B*) opposed-phase images of AML show maintained central hyperintensity (as is also seen with retroperitoneal fat) with India ink artifact at the boundary of the AML and renal parenchyma on opposed-phase image (*arrow*). (*C*) In-phase and (*D*) opposed-phase images in ccRCC show diffuse signal intensity loss on opposed-phase image (*arrows*), indicating microscopic (intracellular) fat not macroscopic (bulk) fat.

As in other areas of the body, when a large mass is first detected, identifying the site of origin can be challenging. For instance, when an AML presents as a large fat-containing retroperitoneal mass, it may be misidentified as a retroperitoneal liposarcoma, as these masses can have a similar appearance. In these cases, an accurate diagnosis is crucial; an AML is benign and may not require therapy, whereas a liposarcoma requires radical resection. Because AMLs arise from the kidney, a defect will be found in the renal parenchyma at the location of origin. AMLs also tend to contain large vessels, whereas sarcomas tend to be hypovascular, and AMLs are often multiple, whereas liposarcomas are a unicentric process (see **Fig. 17**).[44]

Approximately 5% of AMLs contain so few adipocytes that they cannot be discerned on unenhanced CT images or on MR images obtained with fat-suppression techniques; these masses are known as fat-poor AMLs (fpAMLs). The scarcity of fat cells can cause signal intensity loss in a noncurvilinear or diffuse manner on opposed-phase T1-weighted gradient-recalled echo images when compared with in-phase images, indicating the presence of microscopic fat. Microscopic fat, however, can be detected in 2 different settings: from a scarce number of adipocytes (as in fpAML) or from the presence of fat within tumor cells (as can be seen in ccRCC) (**Fig. 18**).[35] This distinction cannot be made with chemical shift imaging alone, and so additional features must be considered to determine the diagnosis. fpAMLs are more common in women and are generally small and hyperattenuating on unenhanced CT images due to a high percentage of smooth muscle component.[36] These masses also tend to be T2 hypointense (T2 signal intensity ratio <0.9) and hyperenhance after contrast administration (arterial-to-delayed enhancement ratio >1.5).[45] These findings are in contradistinction to those seen with pRCC; these masses are T2 hypointense but hypoenhance after contrast administration. The findings are also different from those seen with ccRCCs, which hyperenhance after contrast administration but are T2 hyperintense. Both fpAMLs and pRCCs generally show restricted diffusion.

SUMMARY

Radiologists face several pitfalls when interpreting images of the kidneys. Clinical history is paramount to guiding an appropriate evaluation, and attention to technical details, use of multiplanar imaging, and appropriate use of attenuation measurements can help readers avoid interpretation mistakes. Knowledge of the expected imaging appearance of kidneys after various treatments for RCC and patterns of fat within renal masses and how they impact the differential diagnosis of a focal renal mass will also help to minimize diagnostic errors.

ACKNOWLEDGMENTS

The author thanks Megan Griffiths for her careful review and editing of this article.

DISCLOSURES

None.

REFERENCES

1. Barrett JF, Keat N. Artifacts in CT: recognition and avoidance. Radiographics 2004;24(6):1679–91.
2. Johnson PT, Horton KM, Fishman EK. How not to miss or mischaracterize a renal cell carcinoma: protocols, pearls, and pitfalls. AJR Am J Roentgenol 2010;194(4):W307–15.
3. Wildman-Tobriner B, Allen BC, Maxfield CM. Common resident errors when interpreting computed tomography of the abdomen and pelvis: a review of types, pitfalls, and strategies for improvement. Curr Probl Diagn Radiol 2019;48(1):4–9.
4. Szolar DH, Kammerhuber F, Altziebler S, et al. Multiphasic helical CT of the kidney: increased conspicuity for detection and characterization of small (< 3-cm) renal masses. Radiology 1997;202(1):211–7.
5. Cohan RH, Sherman LS, Korobkin M, et al. Renal masses: assessment of corticomedullary-phase and nephrographic-phase CT scans. Radiology 1995;196(2):445–51.
6. Sheth S, Fishman EK. Multi-detector row CT of the kidneys and urinary tract: techniques and applications in the diagnosis of benign diseases. Radiographics 2004;24(2):e20.
7. Israel GM, Bosniak MA. How I do it: evaluating renal masses. Radiology 2005;236(2):441–50.
8. Rosenkrantz AB, Matza BW, Portnoy E, et al. Impact of size of region-of-interest on differentiation of renal cell carcinoma and renal cysts on multi-phase CT: preliminary findings. Eur J Radiol 2014;83(2):239–44.
9. O'Connor SD, Pickhardt PJ, Kim DH, et al. Incidental finding of renal masses at unenhanced CT: prevalence and analysis of features for guiding management. AJR Am J Roentgenol 2011;197(1):139–45.
10. O'Connor SD, Silverman SG, Ip IK, et al. Simple cyst-appearing renal masses at unenhanced CT: can they be presumed to be benign? Radiology 2013;269(3):793–800.
11. Schieda N, Vakili M, Dilauro M, et al. Solid renal cell carcinoma measuring water attenuation (-10 to 20

HU) on unenhanced CT. AJR Am J Roentgenol 2015;205(6):1215–21.
12. O'Connor SD, Silverman SG, Cochon LR, et al. Renal cancer at unenhanced CT: imaging features, detection rates, and outcomes. Abdom Radiol (NY) 2018;43(7):1756–63.
13. Herts BR, Coll DM, Novick AC, et al. Enhancement characteristics of papillary renal neoplasms revealed on triphasic helical CT of the kidneys. AJR Am J Roentgenol 2002;178(2):367–72.
14. Egbert ND, Caoili EM, Cohan RH, et al. Differentiation of papillary renal cell carcinoma subtypes on CT and MRI. AJR Am J Roentgenol 2013;201(2):347–55.
15. Young JR, Margolis D, Sauk S, et al. Clear cell renal cell carcinoma: discrimination from other renal cell carcinoma subtypes and oncocytoma at multiphasic multidetector CT. Radiology 2013;267(2):444–53.
16. Corwin MT, Loehfelm TW, McGahan JP, et al. Prevalence of Low-Attenuation Homogeneous Papillary Renal Cell Carcinoma Mimicking Renal Cysts on CT. AJR Am J Roentgenol 2018;211(6):1259–63.
17. McGahan JP, Sidhar K, Fananapazir G, et al. Renal cell carcinoma attenuation values on unenhanced CT: importance of multiple, small region-of-interest measurements. Abdom Radiol (NY) 2017;42(9):2325–33.
18. Jonisch AI, Rubinowitz AN, Mutalik PG, et al. Can high-attenuation renal cysts be differentiated from renal cell carcinoma at unenhanced CT? Radiology 2007;243(2):445–50.
19. Smith AD, Remer EM, Cox KL, et al. Bosniak category IIF and III cystic renal lesions: outcomes and associations. Radiology 2012;262(1):152–60.
20. Brinker DA, Amin MB, de Peralta-Venturina M, et al. Extensively necrotic cystic renal cell carcinoma: a clinicopathologic study with comparison to other cystic and necrotic renal cancers. Am J Surg Pathol 2000;24(7):988–95.
21. Kang SK, Huang WC, Panharipande PV, et al. Solid renal masses: What the numbers tell us. AJR Am J Roentgenol 2014;202:1196–206.
22. Kim NY, Lubner MG, Nystrom JT, et al. Utility of CT Texture analysis in differentiating low-attenuation renal cell carcinoma from cysts: A bi-Institutional retrospective study. AJR Am J Roentgenol 2019;213(6):1259–66.
23. Silverman SG, Israel GM, Trinh QD. Incompletely characterized incidental renal masses: emerging data support conservative management. Radiology 2015;275(1):28–42.
24. Agochukwu N, Huber S, Spektor M, et al. Differentiating Renal Neoplasms From Simple Cysts on Contrast-Enhanced CT on the Basis of Attenuation and Homogeneity. AJR Am J Roentgenol 2017;208(4):801–4.
25. Corwin MT, Hansra SS, Loehfelm TW, et al. Prevalence of solid tumors in incidentally detected homogeneous renal masses measuring >20 HU on portal venous phase CT. AJR Am J Roentgenol 2018;211(3):W173–7.
26. Hu E, Ellis JH, Silverman SG, et al. Expanding the definition of a benign renal cyst on contrast-enhanced CT: can incidental homogeneous renal masses measuring 21-39 HU be safely ignored? Acad Radiol 2018;25(2):209–12.
27. Mir MC, Ercole C, Takagi T, et al. Decline in renal function after partial nephrectomy: etiology and prevention. J Urol 2015;193(6):1889–98.
28. Dong W, Zhang Z, Zhao J, et al. Excised parenchymal mass during partial nephrectomy: functional implications. Urology 2017;103:129–35.
29. Pai D, Willatt JM, Korobkin M, et al. CT appearances following laparoscopic partial nephrectomy for renal cell carcinoma using a rolled cellulose bolster. Cancer Imaging 2010;10:161–8.
30. Sarwani NI, Motta-Ramirez GA, Remer EM, et al. Imaging findings after minimally invasive nephron-sparing renal therapies. Clin Radiol 2007;62(4):333–9.
31. Hecht EM, Bennett GL, Brown KW, et al. Laparoscopic and open partial nephrectomy: frequency and long-term follow-up of postoperative collections. Radiology 2010;255(2):476–84.
32. Kshirsagar AV, Choyke PL, Linehan WM, et al. Pseudotumors after renal parenchymal sparing surgery. J Urol 1998;159(4):1148–51.
33. Lee MS, Oh YT, Han WK, et al. CT findings after nephron-sparing surgery of renal tumors. AJR Am J Roentgenol 2007;189(5):W264–71.
34. American Urological Association. Follow-up for clinically localized renal neoplasms guidelines. 2013. Avaialble at: https://www.auanet.org/guidelines/renal-cancer-follow-up-for-clinically-localized-renal-neoplasms-guideline. Accessed November 25, 2019.
35. Tubre RW, Parker WP, Dum T, et al. Findings and impact of early imaging after partial nephrectomy. J Endourol 2017;31(3):320–5.
36. Lang EK, Thomas R, Davis R, et al. Multiphasic helical CT criteria for differentiation of recurrent neoplasm and desmoplastic reaction after laparoscopic resection of renal mass lesions. J Endourol 2004;18(2):167–71.
37. Allen BC, Remer EM. Percutaneous cryoablation of renal tumors: patient selection, technique, and post-procedural imaging. Radiographics 2010;30(4):887–902.
38. Javadi S, Ahrar JU, Ninan E, et al. Characterization of contrast enhancement in the ablation zone immediately after radiofrequency ablation of renal tumors. J Vasc Interv Radiol 2010;21(5):690–5.
39. Porter CA 4th, Woodrum DA, Callstrom MR, et al. MRI after technically successful renal cryoablation:

early contrast enhancement as a common finding. AJR Am J Roentgenol 2010;194(3):790–3.
40. Takaki H, Nakatsuka A, Cornelis F, et al. False-positive tumor enhancement after cryoablation of renal cell carcinoma: a prospective study. AJR Am J Roentgenol 2016;206(2):332–9.
41. Schieda N, Davenport MS, Pedrosa I, et al. Renal and adrenal masses containing fat at MRI: Proposed nomenclature by the Society of Abdominal Radiology Disease-focused Panel on Renal Cell Carcinoma. J Magn Reson Imaging 2019;49(4):917–26.
42. Jinzaki M, Silverman SG, Akita H, et al. Renal angiomyolipoma: a radiological classification and update on recent developments in diagnosis and management. Abdom Imaging 2014;39(3):588–604.
43. Schieda N, Avruch L, Flood TA. Small (<1 cm) incidental echogenic renal cortical nodules: chemical shift MRI outperforms CT for confirmatory diagnosis of angiomyolipoma (AML). Insights Imaging 2014;5(3):295–9.
44. Israel GM, Bosniak MA. Pitfalls in renal mass evaluation and how to avoid them. Radiographics 2008;28(5):1325–38.
45. Sasiwimonphan K, Takahashi N, Leibovich BC, et al. Small (<4 cm) renal mass: differentiation of angiomyolipoma without visible fat from renal cell carcinoma utilizing MR imaging. Radiology 2012;263(1):160–8.